Int J Adv Manuf Technol (2016) 82:901–907
DOI 10.1007/s00170-015-7450-2

ORIGINAL ARTICLE

Optimization of laser micromachining process for biomedical device fabrication

L. Giorleo[1] · E. Ceretti[1] · C. Giardini[2]

Received: 16 March 2015 / Accepted: 15 June 2015 / Published online: 27 June 2015

Abstract Laser machining is commonly used for fabrication of medical devices with microscale features, including vascular stents, drug delivery devices, and scaffolds for tissue engineering with controlled pore size and porosity. The process can also be used to produce structured scaffolds for controlling cell growth, orientation, and location. Moreover, lasers may be used to fabricate complex channel nets in which cells are subsequently seeded or to pattern channels for microfluidic devices. Traditionally, these micro devices were fabricated using silicon substrates, but recently the use of titanium allowed to produce more robust devices at a reasonable cost. In particular, the high quality surfaces that can be obtained with laser machining reduce the liquid flow turbulence and avoid micro cavities formation, critical for bacteria proliferation. The present research reports the results of an investigation on the process capability of laser ablation to produce micro pockets fabricated on titanium sheet (0.5 mm thick). A first experimental campaign was designed for identifying a set of laser ablation cycles able to realize the micro pockets by changing the process parameters as scanning speed, laser power, q-switch frequency, loop number, and duty cycle. Moreover, a process optimization was executed in order to produce the pockets with a highly flat surface. The results were acquired by a confocal laser scanning microscope (CLSM) to obtain high-resolution images with depth selectivity and were analyzed with statistic methods for the identification of the best parameter configuration.

Keywords Laser micromachining · Surface analysis · Titanium

1 Introduction

Surfaces act as interfaces governing the functional behavior of a product. Often, the behavior controlling mechanisms involve surface details on a micrometer or nanometer scale. Many emerging products are based on achieving these small scales, as the case of precision engineering, micro engineering, and nanotechnology [1]. This assumption finds broad consensus in medical device industry where surfaces are the primary place of contact between biomaterial and organism; in this environment, the need for designing and manufacturing materials to make them highly compatible with living tissue (including bio fluids such as blood) has become a major priority [2].

The manufacturing technologies related to surface machining have been constantly improved in order to fulfill the requirements of medical device industry: nowadays, a downscaling of several processes such as machining, molding, or EDM is needful to produce micro workpieces used in biomedical applications [3].

However, despite the improvements of the mentioned processes, with higher demand for evermore sophisticated micro features generated in a variety of materials, pulsed laser ablation has become a key technology for high-added-value industries. Moreover, the need for micro- and nano-manufacturing is dictated not only by the requirement of

✉ L. Giorleo
luca.giorleo@unibs.it

E. Ceretti
elisabetta.ceretti@unibs.it

C. Giardini
claudio.giardini@unibg.it

[1] Dept. of Mechanical and Industrial Engineering, University of Brescia, Brescia, Italy

[2] Dept. of Management, Information and Production Engineering, University of Bergamo, Bergamo, Italy

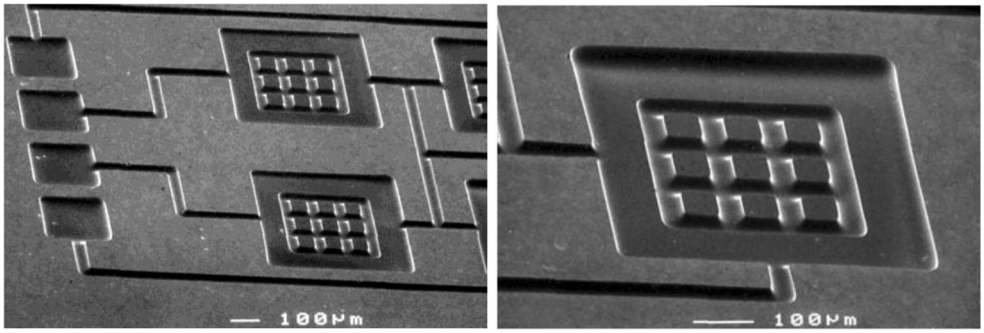

Fig. 1 Two-level titanium microstructure designed for microfluidic applications [8]

increasingly sophisticated devices and structures with novel properties but also by the trend of decreasing component sizes, material usage, and energy consumption of products [4, 5].

For the described reasons, laser machining aims to become commonly used for the fabrication of medical devices with microscale features, including vascular stents, drug delivery devices, and scaffolds for tissue engineering with controlled pore size and porosity. This process can also be used to produce structured scaffolds for controlling cell growth, orientation, and location or for fabricating complex channel nets where cells are subsequently seeded. Laser machining may also be used to pattern channel microfluidic devices. Traditionally, these micro devices have been fabricated using silicon substrates, but ongoing research activities report the use of titanium to fabricate microfluidic networks. Compared with silicon, glass, and polymers, titanium is a metal with high strength and excellent biocompatibility.

Titanium biocompatibility comes from the spontaneous formation, in air and blood, of a highly biocompatible dioxide passivation film, which prevents corrosion in fluid environments and guarantees long-term implant lifetime. The high strength of titanium together with its biocompatibility provides many advantages when using this material for microfluidic applications. Moreover, these titanium devices were found to be more robust than their silicon counterparts and can be fabricated in such a way that X-ray attenuation is reduced or eliminated during small-angle X-ray scattering experiments (used for example in protein detection) [6, 7]. At the same time, a high-quality machining is fundamental in device fabrication; in particular, referring to the bottom surface quality, it should be as flatter as possible in order to avoid any turbulence of the liquid flow or the generation of micro cavities that could be critical for storage of bacteria. In Fig. 1, an example of titanium microfluidic device is reported [8].

In literature, many authors focused their researches in enhancing knowledge about laser micromachining process [9, 10] and its application for different medical devices' fabrication [11, 12] on different materials as PMMA materials [13] or titanium [14] with femto [15] and nano [16] laser pulse using UV [17] or Nd:YAG wavelength [18].

In order to enhance the knowledge about this topic, the present research reports the results of an investigation on

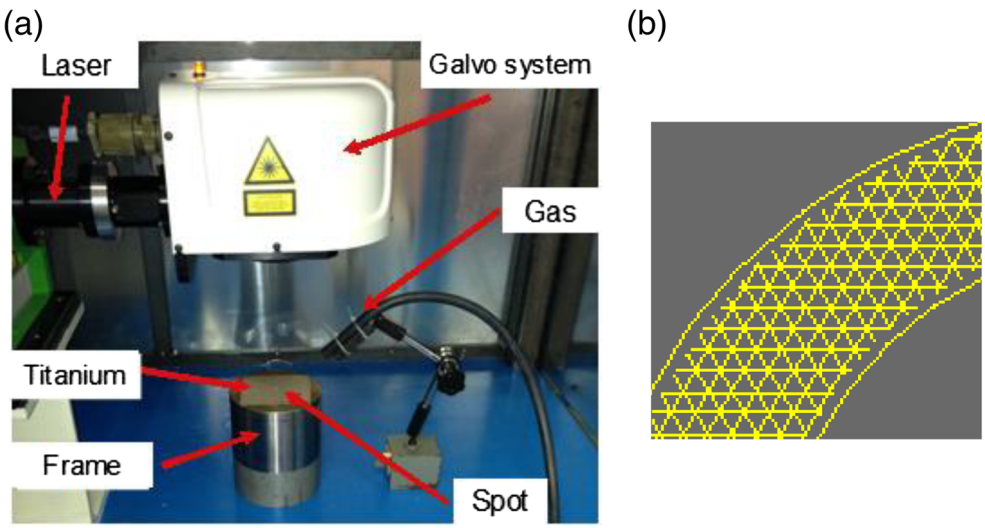

Fig. 2 **a** Setup of the experiments and **b** laser path net three-line filling strategy

Table 1 Direct and indirect laser parameters

Symbol	Description	Equation
L [mm]	Sample length	0.5
A [mm^2]	Sample area	0.25
f [kHz]	q-switch frequency	30,100
P_{avg} [W]	Average power	2.64, 1.45, 0.35
v_s [mm/s]	Scan speed	381, 304.8, 228.6
d [mm]	Spot diameter	0.1
abs [%]	Absorption coefficient [20]	50
dt [ns]	Pulse width	$\mathrm{dt} = \frac{\mathrm{duty\ \ cycle}}{f}$
P_{peak} [W]	Peak power	$P_{peak} = \frac{P_{avg}}{f \times \mathrm{dt}}$
t_{loop} [s]	Time per loop	$t_{loop} = 3\frac{A}{d}\frac{1}{V_s}$
ov	Pulses overlap	$\mathrm{ov} = 1 - \frac{V_s}{d \times f}$
n_{scan}	Number of scans	$n_{scan} = \frac{L}{D}$
n_{pulse}	Number of pulses	$n_{pulse} = 3n_{scan}\left[1 + \frac{L-d}{(1-\mathrm{ov})d}\right]$
E_{pulse} [J]	Energy per pulse	$E_{pulse}=P_{peak}\mathrm{dt}$
E_{loop} [J]	Energy per loop	$E_{loop}=P_{peak}\mathrm{dt}$
F_{pulse} [J/cm^2]	Fluence per pulse	$F\mathrm{pulse} = \mathrm{abs}\frac{4}{\pi d^2}E_{pulse}$

the process capability of laser ablation to produce micro pockets fabricated on titanium sheet (0.5 mm thick). A first experimental campaign was designed for identifying a set of laser ablation cycles able to realize the micro pockets by changing the process parameters as scanning speed, laser power, q-switch frequency, loop number, and duty cycle. Moreover, a process optimization was executed in order to produce the pockets with a highly flat surface. The results were acquired by a confocal laser scanning microscope (CLSM) to obtain high-resolution images with depth selectivity and were analyzed with statistic methods for the identification of the best parameter configuration.

Table 2 Designed laser machining cycle

Process parameters	Roughing (R)	Finishing (F)	Polishing (P)
v_s [mm/s]	304.8	228.6	381
f [kHz]	30	30	100
Duty cycle [%]	30	30	100
dt [ns]	10^4	10^4	–
P_{peak} [W]	8.80	4.83	0.35
F_{pulse} [J/cm^2]	0.56	0.31	0.22
No. of loop	25	8	20
t [s]	0.62	0.26	0.39
E [J]	1.33	0.31	0.11

1.1 Modeling setup

The setup of the experiment is reported in Fig. 2a. A LEP Lee Laser (Nd:YVO4, 8 W q-switched, λ= 532 nm) was used for the experimental campaign. The outgoing laser beam is collimated in a galvo system to impose a remote control. A sheet of titanium grade 2 (0.5 mm thick) was selected as sample. The sheet was fixed on a frame at a distance equal to the focal distance (160 mm) from the galvo head. Nitrogen was chosen as assist gas; the gas feeding was realized with a tube fixed on a support to obtain a homogeneous flux oriented at 45° with respect to the specimen.

The laser machine is controlled by a software, and it is possible to set the scan speed, the q-switch frequency, the duty cycle (i.e., the product between the frequency and the pulse width), the laser path strategy, the beam diameter, the loop number, and the laser power expressed as the percentage of the applied current to the pump system (diode lasers). A preliminary calibration curve with a power meter (Gentec-EO UP19-W)

was executed to convert the percentage ampere in average power. Based on a previous experience [19], the laser path was imposed equal to the net three-line filling strategy as reported in Fig. 2b.

The campaign results were analyzed not only with regard to the obtained geometries but also as a function of time and energy needed to realize them. These parameters must be evaluated as indirect measures: Table 1 reports the equations necessary for evaluating the energy and the time per loop. To test if the power density is able to ablate the titanium or not, the fluence per pulse was evaluated too. The constant 3 present in time per loop and number of pulses equations was included taking into account the imposed net three-line laser path strategy.

Following the mentioned setup, different tests were executed for studying the laser machining process performance. For each test, a micro pocket sample with a dimension equal to 500×500 μm^2 was realized on the titanium grade 2 samples. The obtained pocket depth was determined by the process parameters set and in the range between 50 and 100 μm typical of microfluidic devices.

The method designed to obtain the pocket sample with a laser beam was chosen coherently with a standard milling process: three different machining cycles were executed on the sample surface; each cycle was characterized by a different set of process parameters in order to perform a roughing (R), finishing (F), and polishing (P) cycle. The polishing cycle was designed imposing a duty cycle equal to 100 % that correspond to a continuous laser mode. Each cycle was repeated for several loops to obtain the desired pocket depth. Table 2 summarizes the designed experiments. In Table 2, the total time (t) and energy (E) needed for each cycle were introduced; they were evaluated as the product of t_{loop} and E_{loop} for the loop numbers. As it can be observed, each cycle reaches a fluence per pulse value higher than 0.109 J/cm^2: the ablation threshold for titanium alloy [21].

Table 3 Pocket depth and laser machining quality results

Test	N_2 [bar]	t [s]	E [J]	No. of loop			Depth [μm]		σ_{bottom}
				(R)	(F)	(P)	μ_{depth}	σ_{depth}	
1	0	0.62	1.33	25	0	0	66.77	11.11	3.41
2	0	0.26	0.31	0	8	0	7.43	2.03	0.82
3	0	0.39	0.11	0	0	20	0.05	1.15	0.57
4	0	0.88	1.64	25	8	0	72.76	8.78	2.74
5	0	1.27	1.75	25	8	20	75.34	8.97	2.10
6	5	0.62	1.33	25	0	0	91.05	15.37	8.46
7	5	0.26	0.31	0	8	0	8.84	2.67	1.35
8	5	0.39	0.11	0	0	20	0.11	1.13	0.52
9	5	0.88	1.64	25	8	0	87.36	12.98	5.44
10	5	1.27	1.75	25	8	20	88.71	13.04	4.24

Under these hypotheses, ten tests were carried out to study the single and the cumulative laser cycle effects. The assist gas influence was analyzed, too.

2 Main results

The obtained pocket geometries were acquired by a CLSM to obtain high-resolution images with depth selectivity. The Olympus LEXT OLS4100 microscope equipped with a ×200 objective was used for the profile acquisition in order to have a resolution equal to 0.625 μm on x and y axis, while the z movement resolution was set equal to 10 nm. Under this configuration, an area equal to 640×640 μm^2 was scanned for each test. The average depth obtained (μ_{depth}) was acquired as the difference between the top and bottom average measures; the top values where acquired on a frame having a width equal to 20 μm (about 12 K points), designed avoiding

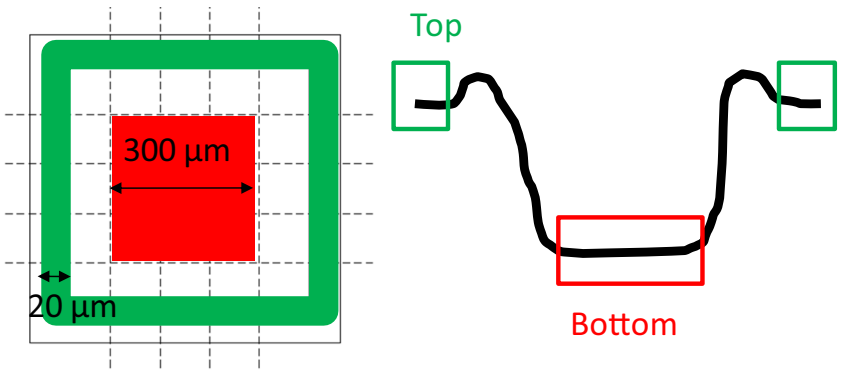

Fig. 3 Strategy adopted for the pocket geometry acquisition

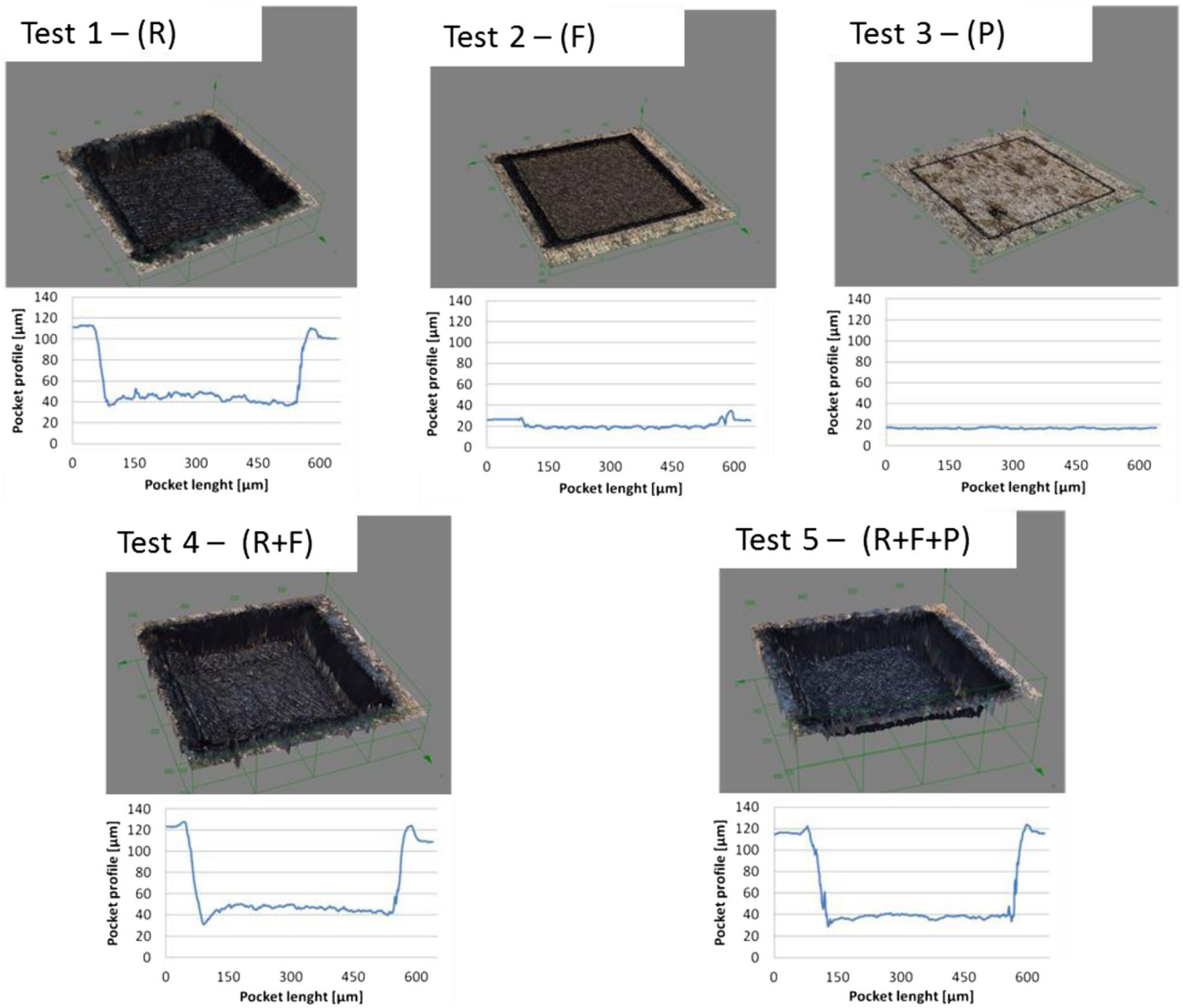

Fig. 4 Single and cumulative laser cycle profiles (no gas tests)

the burrs. The bottom values were selected referring to a 300×300 µm^2 area in the middle of the pocket (about 230 K points). The standard deviation (σ_{depth}) was evaluated as the sum of the standard deviations of the top and bottom surface according to the error propagation theory. In Fig. 3, the strategy adopted for geometry acquisition is plotted.

To analyze the process performance, the bottom standard deviation was taken into account. The equations for the depth estimation parameter are reported in the following:

$$\mu_{depth} = \mu_{top} - \mu_{bottom}$$

$$\sigma_{depth} = \sigma_{top} + \sigma_{bottom}$$

Starting from these formulations, Table 3 reports depth and quality parameters measured for each experiment. Moreover, examples of high-resolution images acquired with the confocal laser microscope are shown in Fig. 4 where the pocket profile referred to a middle section is plotted too.

Table 4 Optimization campaign results

No. of loop (F)	t [s]	E [J]	σ_{bottom}		Depth [µm]
			μ_{depth}	σ_{depth}	
8	0.26	0.31	7.43	2.03	0.82
68	2.23	2.64	66.16	5.95	1.61
83	3.12	3.33	118.37	12.13	2.65
107	3.90	4.26	149.37	11.65	4.63
115	3.77	4.46	171.48	12.92	5.72

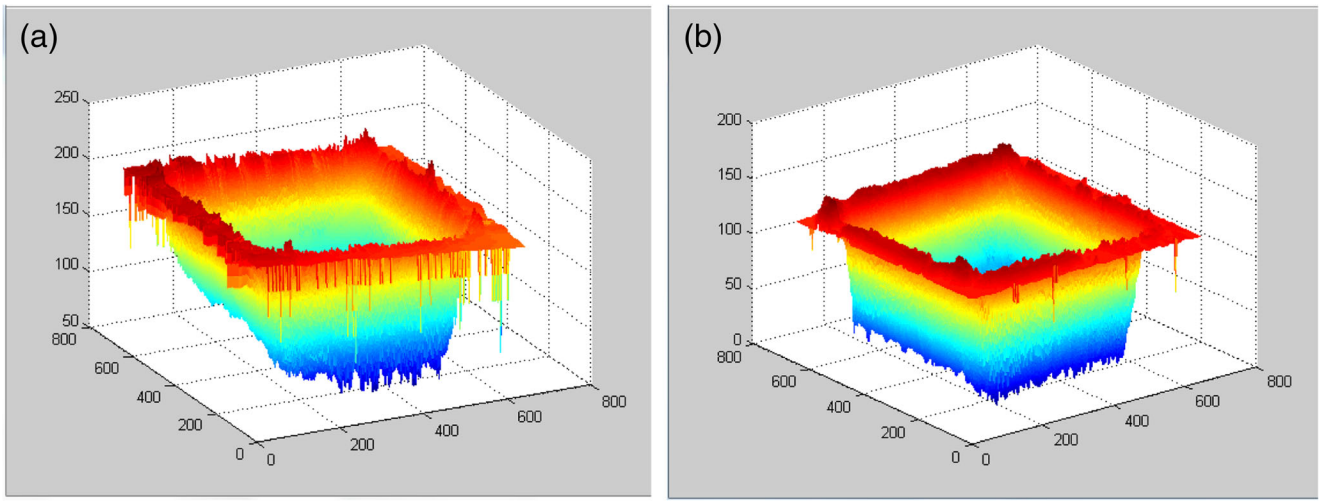

Fig. 5 Qualitative comparison between test 10 (**a**) and test 11 (**b**)

Analyzing the results, it is possible to draw the following considerations:

- as expected, the roughness, finishing, and polishing cycles were characterized by a decreasing amount of ablated material and by an increase of surface quality.
- a similar consideration is evident for the energy (higher in R, lower in P) while considering the execution time, the finishing cycle is the fastest one.
- the assist gas effect guarantees an inert area surrounding the ablation process and it results in benefits in terms of vaporized depth, while on the contrary, the gas stream generates a turbulence that worsts the surface quality (tests from 1–5 with respect to tests 6–10). However, an inert process is always preferred to avoid oxidization phenomena.

Starting from the obtained results, a further investigation was designed to improve the process performance in terms of surface quality. The experimental campaign was focused on the estimation of a regression model able to predict the pocket depth as a function of the loop number. In this campaign, only the finishing cycle with assist gas was taken into account because of the previous considerations (the roughness cycle and the assist gas highly worsen the surface quality and the polishing cycle becomes negligible when the irradiated surface is out of the focus distance). Table 4 highlights the results of the designed optimization campaign.

Table 5 Quantitative comparison between test 10 and test 11

Test	t [s]	E [J]	Depth [μm]		σ_{bottom}
			μ_{depth}	σ_{depth}	
10	1.27	1.75	88.71	13.04	4.24
11	2.46	2.91	88.19	7.31	2.21

The estimated regression model is as follows:

$$\mu_{depth} = 1.27 + 0.596 \cdot loop + 0.007706 \cdot loop^2$$

The correlation coefficient R^2 is equal to 98 %, proving a good agreement between experimental and fitted values. The hypotheses of the homogeneity of variance and normality of residuals are verified too. Finally, the regression model was used for carrying out a new test (test 11), imposing a loop number equal to 75 that corresponds to an estimated depth equal to 89 μm in order to be comparable with test 10 results. In Fig. 5 and Table 5, the obtained geometry and the main results are respectively reported.

As it can be observed, the new approach allows the realization of a pocket having the same depth but with an almost doubled surface quality (σ_{bottom}). On the other hand, the machining time and the needed energy double too.

3 Conclusions

In the present paper, the performance of a laser machining process executed with a 532-nm q-switched laser has been studied and discussed for microfluidic device fabrication. Several micro pockets with depth in the range between 50 and 100 μm have been realized on titanium sheets. The results were acquired by a CLSM to obtain high-resolution images with depth selectivity and were analyzed with statistic methods. The process designed to obtain the pocket sample with a laser beam was chosen coherent with a typical milling process: three different machining cycles, roughing, finishing, and polishing, were executed achieving good quality results

considering the realized pocket bottom surface. To improve process performance, a regression model based on the finishing cycle was estimated. The model proved to be able to improve the bottom surface quality. Further experiments are now under study for optimizing the process performance.

References

1. De Chiffre L, Kunzmann H, Peggs GN, Lucca DA (2003) Surfaces in precision engineering, microengineering and nanotechnology. CIRP Ann 52(2):561–577. doi:10.1016/S0007-8506(07)60204-2
2. Ramsden JJ, Allen DM, Stephenson DJ, Alcock JR, Peggs GN, Fuller G, Goch G (2007) The design and manufacture of biomedical surfaces. CIRP Ann 56(2):687–711. doi:10.1016/j.cirp.2007.10.001
3. Masuzawa T (2000) The state of art of micromachining. CIRP Ann 49(2):473–488. doi:10.1016/S0007-8506(07)63451-9
4. Li L, Hong M, Schmidt M, Zhong M, Malshe A, Huis in'tVeld B, Kovalenko V (2011) Laser nano-manufacturing—state of the art and challenges. CIRP Ann 60:735–755. doi:10.1016/j.cirp.2011.05.005
5. Meijer J, Du K, Gillner A, Hoffmann D, Kovalenko VS, Masuzawa T, Ostendorf A, Poprawe R, Schulz W (2002) Laser machining by short and ultrashort pulses, state of the art and new opportunities in the age of the photons. CIRP Ann 51(2):531–550. doi:10.1016/S0007-8506(07)61699-0
6. Parker ER, Hirst LS, Safinya CR, MacDonald NC (2005) Bulk titanium microfluidic networks for protein self-assembly studies. Proceedings of MicroTAS 2005 Conference: 9th International Conference on Miniaturized Systems for Chemistry and Life Sciences 1: 945–947. http://www.engineering.ucsb.edu/~memsucsb/Research/publications/parker_microtas05.pdf. Accessed 5 May 2015
7. Meinhart C, MacDonald N, Mezic I, Saffinya C (2005) Titanium-based biomolecular manipulation tools, NSF Nanoscale Science and Engineering Grantees Conference. http://www.nseresearch.org/2005/NewFiles/ov16_0404444UCSB_Meinhart.pdf. Accessed 5 May 2015
8. http://micropat.ch/application/titanium-microfluidic. Accessed 5 May 2015
9. Campanelli SL, Ludovico AD, Bonserio C, Cavalluzzi P, Cinquepalmi M (2007) Experimental analysis of the laser milling process parameters. J Mater Process Technol 191:220–223. doi:10.1016/j.jmatprotec.2007.03.005
10. Garnov SV, Konov VI, Kononenko T, Pashinin VP, Sinyavsky MN (2004) Microsecond laser material processing at 1.06 nm. Laser Physics 14:910–915. http://www.maik.ru/full/lasphys_archive/04/6/lasphys6_04p910full.pdf. Accessed 5 May 2015
11. Liu X, Chu PK, Ding C (2004) Surface modification of titanium, titanium alloys, and related materials for biomedical applications. Mater Sci Eng 47:49–121. doi:10.1016/j.mser.2004.11.001
12. Chen K, Yao YL (2000) Process optimization in pulsed laser micromachining with applications in medical device manufacturing. Int J Adv Manuf Technol 16:243–249. doi:10.1007/s001700050152
13. Teixidor D, Thepsonthi T, Ciurana J, Özel T (2012) Nanosecond pulsed laser micromachining of PMMA-based microfluidic channels. J Manuf Process 14:435–442. doi:10.1016/j.jmapro.2012.09.001
14. Fasasi AY, Mwenifumbo S, Rahbar N, Chen J, Li M, Beye AC, Arnold CB, Soboyejo WO (2009) Nano-second UV laser processed micro-grooves on Ti6Al4V for biomedical applications. Mater Sci Eng C 29:5–13. doi:10.1016/j.msec.2008.05.002
15. Zhao J, Huettner B, Menschig A (2001) Microablation with ultrashort laser pulses. Opt Laser Technol 33:487–491. doi:10.1016/S0030-3992(01)00066-4
16. Gittard SD, Narayan RJ (2010) Laser direct writing of micro- and nano-scale medical devices. Expert Rev Med Devices 7(3):343–356. doi:10.1586/erd.10.14
17. Yasa E, Kruth JP (2010) Investigation of laser and process parameters for selective laser erosion. Precis Eng 34:101–112. doi:10.1016/j.precisioneng.2009.04.001
18. Chen TC, Darling RB (2008) Laser micromachining of the materials using in microfluidics by high precision pulsed near and mid-ultraviolet Nd:YAG lasers. J Mater Process Technol 198:248–253. doi:10.1016/j.jmatprotec.2007.06.083
19. Giorleo L., Ceretti E., Giardini C. (2014) Ti surface laser polishing: effect of laser path and assist gas, 9th CIRP Conference on Intelligent Computation in Manufacturing Engineering - CIRP ICME '14, Capri, Italy, July, 23–25.
20. Tang G, Abdolvand A (2013) Structuring of titanium using a nanosecond-pulsed Nd:YVO4 laser at 1064 nm. Int J Adv Manuf Technol 66:1769–1775. doi:10.1007/s00170-012-4456-x
21. Zheng B, Jiang G, Wang W, Wang K, Mei X (2014) Ablation experiment and threshold calculation of titanium alloy irradiated by ultra-fast pulse laser. AIP Adv 4:1–9. doi:10.1063/1.4867088